Acta Biomaterialia 6 (2010) 319–330

Contents lists available at ScienceDirect

Acta Biomaterialia

journal homepage: www.elsevier.com/locate/actabiomat

Microstructure, elastic properties and deformation mechanisms of horn keratin

Luca Tombolato [a], Ekaterina E. Novitskaya [a], Po-Yu Chen [b], Fred A. Sheppard [a], Joanna McKittrick [a,b,*]

[a] Department of Mechanical and Aerospace Engineering, University of California, San Diego, La Jolla, CA 92093-0411, USA
[b] Materials Science and Engineering Program, University of California, San Diego, La Jolla, CA 92093-0418, USA

ARTICLE INFO

Article history:
Received 16 February 2009
Received in revised form 26 June 2009
Accepted 29 June 2009
Available online 3 July 2009

Keywords:
Keratin
Sheep horn
Mechanical properties
Microstructure
Lamellar composite

ABSTRACT

The structure and mechanical properties of the horns from a desert bighorn sheep, *Ovis canadensis*, were examined. Horns must be strong and durable as they are subjected to extreme loading impacts, making them superior structural materials. Horns are composed of α-keratin, a fibrous, structural protein found in hair, nails, claws and hooves. Horns have a lamellar structure (2–5 μm in thickness) stacked in the radial direction with tubules (~40 × 100 μm in diameter) dispersed between the lamellae, extending along the length of the horn in the growth direction. Compression and bending tests were conducted in both rehydrated and ambient dried conditions. The yield strength and elastic modulus are anisotropic and are correlated with the orientation of the tubules. Rehydrated samples showed significant loss of strength and modulus. Microscopy of fractured samples revealed several toughening mechanisms: delamination and ligament bridging in bending and delamination and microbuckling of the lamellae in compression.

1. Introduction

Porous materials are characterized by a low density. Although mechanical properties such as stiffness, toughness and strength might not be outstanding compared to bulk materials, the low density allows them to attain high specific mechanical properties. Structural biological materials, such as cancellous bone, dentine, bird beaks and feathers, hooves and horns, can be considered porous materials. Over the last few years, structural biological materials have attracted increasing attention from materials researchers. For the most part, this interest has focused on bones [1–3], teeth [4,5], mollusk shells [6–8] and hooves [9–17], elucidating the relationship between structure, mechanical properties, and their mutual interaction. Meyers and co-workers [18,19] have published review articles on the structure and properties of structural biological materials. Horns, on the other hand, which are the subject of this study, have not been examined in detail.

Horns appear on animals from the Bovidae family, which include cattle, sheep, goats, antelope, oryx and waterbuck, and are tough, resilient and highly resistant to impact. In the case of male bighorn sheep, the horns must be strong and durable as they are subjected to extreme loading impacts during the life of the animal and, unlike antlers, will not grow back if broken. Horns are not living tissue – there are no nerves and they do not bleed when fractured. On the living animal, horns encase a short bony core (os cornu) composed of cancellous (spongy or trabecular) bone and covered with skin, which projects from the back of the skull [20]. The horn is not integrated to the skull and can pull away if the hide is removed. The skin covering the bony core is a germinative epithelium that generates new cells to grow the horn. There are quite a variety of horn shapes and sizes, from the stumpy horns on domestic cattle to the extravagant forms seen on the greater kudu (*Tragelaphus strepsiceros*), the blackbuck (*Antilope cervicapra*) and the Nubian ibex (*Capra nubiana*). Unlike other structural biomaterials (e.g. bone, tusk, teeth, antlers, mollusk shells), horn does not have a mineralized component and is composed primarily of α-keratin.

α-Keratin is a structural, fibrous protein found in wool, hair, nails, mammalian claws, equine and bovine hooves, and horns. In α-keratin glycine and alanine, the smallest amino acids, are found in high concentrations. The keratin molecules are held together by H-bonding and disulfide cross-linked bonds, due to the presence of cysteine. The disulfide bridges produce more rigidity in the structure and contribute to the insolubility of keratin. At the lowest level, two polypeptide chains (types I and II) [21,22], which belong to a family of related proteins, form two-strand coiled-coil molecules approximately 45 nm in length and 1 nm in diameter. These molecules are helically wound and assemble into microfibrils (called intermediate filaments, IFs), forming 'superhelical' ropes 7 nm in diameter [23]. The α-helices are mainly parallel to the long axis of the ropes. These IFs are embedded in a viscoelastic protein matrix. This matrix is composed of two types of proteins – high sulfur proteins, which have more cysteinyl residues, and high glycine–tyrosine proteins, which have high contents of glycyl residues [22]. In hooves and the rhinoceros horn, the filaments and the

* Corresponding author. Tel.: +1 858 534 5425; fax: +1 858 534 5698.
E-mail address: jmckittrick@ucsd.edu (J. McKittrick).

1742-7061/$ - see front matter © 2009 Acta Materialia Inc. Published by Elsevier Ltd. All rights reserved.
doi:10.1016/j.actbio.2009.06.033

matrix are further organized into circular lamellae that surround a hollow tubule (medullary cavity), which is similar to the configuration of osteons in compact bone. These lamellar tubules are held together by the intertubular material, which is chemically the same as the tubular material but has a different orientation of IFs [10].

2. Background

Makinson [24] determined that sheep horns consist of flat keratin cells that have faces parallel to the growth direction, with the IFs not completely aligned in the growth direction, but angling off axis by ~20°. Kitchener and co-workers [20,25–29] were the first to provide insights into the fighting behavior of various species in the Bovidae family. Mechanical property measurements (strength, stiffness, work of fracture – see Table 1) revealed that horns are capable of high energy absorption before breaking and hydration is important for decreasing the notch sensitivity. The toughness and work of fracture is higher than for other biological composites, and rivals the properties of bulletproof "glass" (polycarbonate). It was estimated that the maximum fighting force of a bighorn sheep is 3400 N, given the ram's mass and velocity [20,26]. This correlates to compressive and tensile stresses in the horn of 4.0 and 1.4 MPa, respectively. It was further calculated that the critical crack length for crack propagation is ~60% of the transverse dimension of the horn, indicating the superior flaw sensitivity of the material. The specific work of fracture was found to vary along the length of the horn. Fresh waterbuck (*Kobus ellipsiprymnus*) horns were found to range from 10 to 80 kJ m^{-2} and mouflon (*Ovis musimon)* horn ranged from 12 to 60 kJ m^{-2} from the base to the outer tip. The highest work of fracture reported (32 kJ m^{-2}) is greater than most other biological and synthetic materials (antler 6.2 kJ m^{-2}; bone 1.7 kJ m^{-2}; glass 5 J m^{-2}; mild steel >26 kJ m^{-2}) [27]. This was attributed to crack-stopping mechanisms, such as delamination and keratin fiber pullout. Kitchener and Vincent [28] examined the effect of hydration on the elastic modulus of horns from the oryx (*Oryx gazella*). They considered the structure of the horn as a chopped fiber composite, where the crystalline α-keratin fibers (40 nm long) were embedded in an amorphous keratinous matrix. Applying the Voigt model and using a chopped fiber composite analysis with a volume fraction of fibers as 0.61, they predicted a value of the elastic modulus close to the experimental value, indicating that a fibrous composite model of horn keratin is a reasonable assumption. The elastic and shear modulus decreased significantly with an increase in the moisture content [28,29]. The keratin fibers were not affected; rather, the matrix swelled with the water, which decreased the elastic and shear moduli. Warburton [30] had earlier determined that moisture in a sheep horn severely decreased its elastic modulus, with 20 wt.% water reducing it by as much as 75% compared with dry horn.

Hooves are the most similar biological material to horns and have the largest body of scientific literature. Hooves contain tubules ~220 × 140 μm in major and minor axis, respectively, with a medullary cavity of ~50 μm. These tubules are oriented in the longitudinal direction (parallel to the leg). The keratin forms in circular lamellae (~5–15 μm thick) surrounding the tubules [10]. It was concluded that the tubules serve only a mechanical function – to increase crack defection, thereby increasing the toughness, making the equine hoof a highly fracture-resistant biological material [10,15]. Hooves must support large compressive and impact loads and provide some shock absorption from the impact. The most thorough studies have been from Gosline and co-workers [9–11,13,15]. The hoof keratin is described as a nanoscale

Table 1
Comparison of mechanical properties of keratinized materials and other biological and synthetic materials.

	Elastic modulus (GPa)	Tensile strength (MPa)	Bending strength (MPa)	Toughness (MJ m^{-3})	Work of fracture (kJ m^{-2})	Moisture content (wt.% water)	Ref.
Oryx horn (*Oryx gazella*)	4.3		212		19	na	[20]
	6.1	137				0	[28]
	4.3	122				20	[28]
	1.8	56				40	[28]
Waterbuck horn (*Kobus ellipsiprymnus*)	3.3		245		20	na	[20]
Sheep horn (*Ovis canadensis*)	4.1		228		22	na	[20]
	9					0	[30]
	1.5					20	[30]
	2.20		127.1	56–74		10.6	*
	0.81		39.1	12–18		34.5	*
Bovine hoof	0.4	16.2	14.3			29.9	[12]
Equine hoof	2.6	38.9				18.2	[13]
	0.2		19.4			41% RH	[40]
	0.3–0.6	6.5–9.5				100% RH	[10]
Bovine femur bone		148				Hydrated	[41]
	13.5		246.7		1.7		[42]
Antler bone (*Cervus canadensis*)					6.2	Hydrated	[42]
	7		145				[39]
Red abalone shell (*Haliotis rufescens*)	70			1.24		Hydrated	[7]
		170					[7]
			197				[43]
Fiberglass					90		[44]
	5.9	110					[45]
Polycarbonate	2.4	67			33		[46]
				33			[47]

RH, relative humidity; na, not available.
* This work (longitudinal direction – radial direction).

composite comprising IFs as fiber-oriented reinforcement of a hydrated keratin matrix, as shown in Fig. 1(a). Bertram and Gosline measured the effect of hydration on tensile and fracture properties [13]. They found that the stiffness decreased with hydration, ranging from 14.6 GPa (ambient) to 0.4 GPa (100% relative humidity, RH). Water penetrates the intertubular matrix as will as the amorphous polymer surrounding the keratin fibers, acting as a plasticizer and thereby reducing the density and stiffness of the material [31]. Fracture toughness was found to be at a maximum at 75% RH (22.8 kJ m^{-2}). Fracture toughness was calculated by the J-integral method, which is a way to measure the instantaneous change of energy (dissipated) during fracture per unit of newly created fracture surface area. Kasapi and Gosline [10,11] tested stiffness, tensile strength and work of fracture in fully hydrated conditions, to correlate IF volume fraction and alignment with mechanical properties. They found that the stiffness increased toward the outer hoof wall, ranging from 0.30 GPa at the inner region to 0.56 GPa on the outer surface of the hoof wall, despite the increase in porosity in that direction. The increase in elastic modulus was attributed to an increase in the volume fraction of keratin fibers. Further studies revealed that the stiffness reinforcement was due to the IFs' volume fraction rather than their orientation. In the tubular material, the IFs are aligned in the tubule direction. However, they are aligned more perpendicularly to the tubule direction in the intertubular matrix. These different orientations help resist crack propagation through crack redirection, suggesting that the hoof wall structure evolved to maximize the fracture toughness [11].

Bovine hooves are similar to equine hooves in both structure and properties [12,13], as shown in Table 1. Baillie and Fitford [32] described bovine hoof structure as comprising tubules embedded in intertubular material. Franck et al. [12] tested the tensile, compressive and bending strength and stiffness. They were found to be similar to those for equine hooves, considering the slightly different moisture content. Clark and Petrie [14] found the fracture toughness for the bovine hooves (J-integral 8.5 kJ m^{-2}) to be lower than for the equine ones (J-integral 12.0 kJ m^{-2}) [9].

The structural differences found between the bovine hoof and the equine hoof appears to mainly affect the toughness. The bovine tubule wall is thinner and the keratin cells in the intertubular

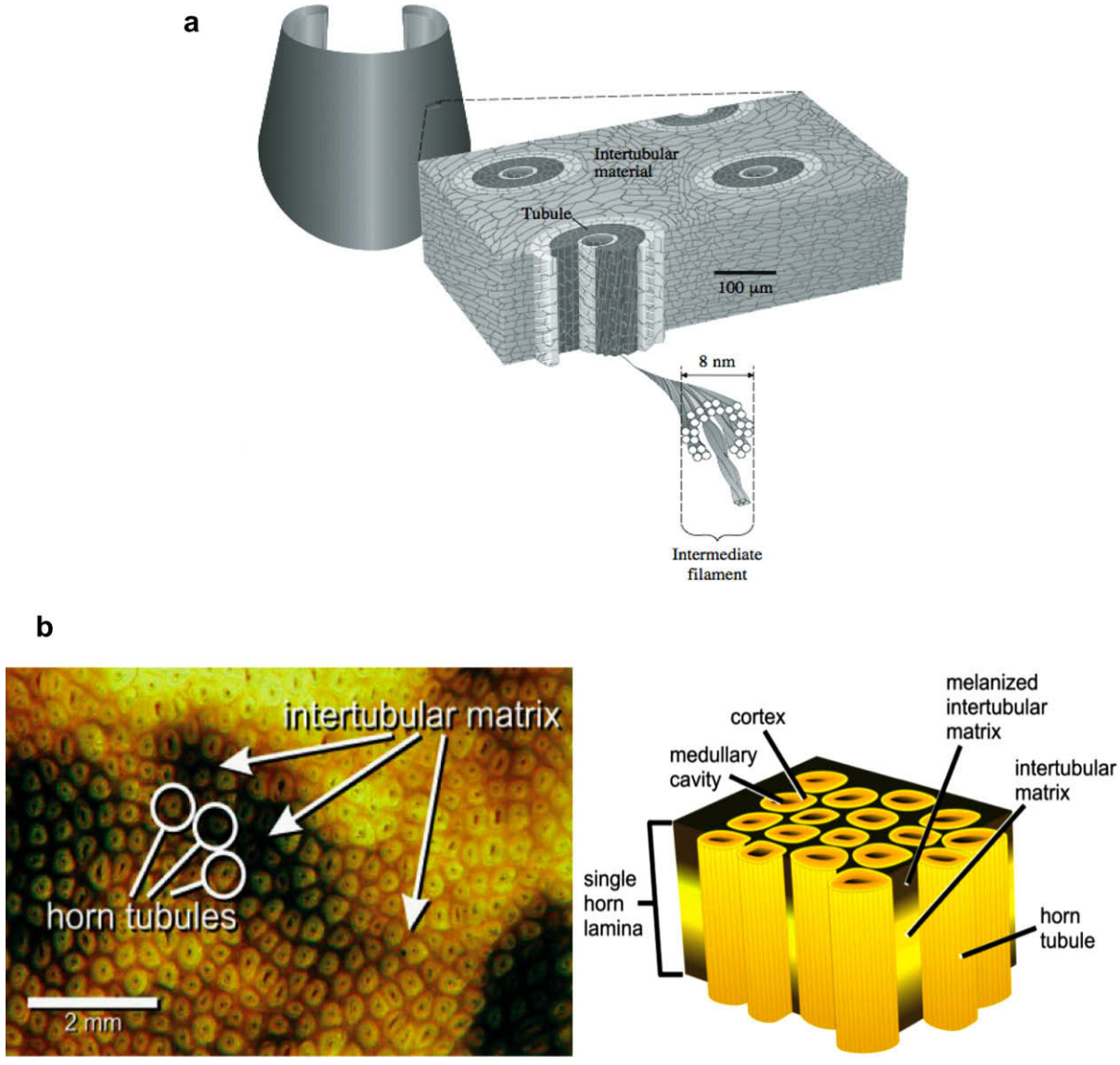

Fig. 1. (a) Illustration of the front view of the equine hoof wall and a sketch of a hoof wall sample showing cells forming tubules and intertubular material. Intermediate filament alignments are drawn on the lamella of the cut-away tubule. Taken from Kasapi and Gosline [11]. (b) Optical micrograph of the white rhinoceros horn, showing tubules and the intertubular matrix. Taken from Hieronymus et al. [34].

material are oriented more parallel to the tubules than the equine hoof. In tandem, the intertubular IFs are aligned more in the direction of the tubules compared to that of the equine hoof. Finally, in the bovine hoof the interaction between tubular and intertubular material appears to be stronger than in the equine hoof, indicating a stronger interface. These differences account for the higher fracture toughness of the equine hoof compared with the bovine hoof.

The rhinoceros horn is another example of biological structural material composed of α-keratin. Ryder [33] observed that the tubules, 300–500 μm in diameter with a medullary cavity of ~20 μm × 60 μm in major and minor axis, respectively, in the horn were slightly coarser than that of equine hoof (20 μm × 40 μm), and there was little intertubular material. Hieronymus et al. [34] found that, unlike the horns of other ungulates, the rhinoceros horn does not have a bony core. Like bovine and equine hooves, rhinoceros horns consist of tubules embedded in the amorphous keratin matrix, as shown in Fig. 1(b). Bendit [17] found the elastic modulus to be strongly dependent on RH, varying from 2 GPa (RH 65%) to 0.03 GPa (RH 100%).

Although the structural properties of bighorn sheep horns are believed to be similar to those of other horns and hooves, as they share the same basic structural protein, a detailed analysis of the structure–property relationships have not been investigated. In fighting force analyses on different bovids, the bighorn sheep was found to be one of the most powerful fighters within this family [26]. Therefore, it is of interest to investigate the microstructural features and mechanical properties that underpin the excellent fracture resistance of their horns. Some mechanical properties have been reported for several species [25]; however, the microstructure, mechanical properties at different orientations, compressive properties and failure mechanisms have not been examined, which is the purpose of this study. Horns are lightweight, tough materials, and biomimetic design based on these structures could result in superior impact-resistant materials.

3. Materials and methods

The bighorn sheep (*Ovis canadensis*) horns were purchased from Into the Wilderness Trading Company (Pinedale, WY). The pair of horns were ~60 cm in length, with the thickest cross-sectional diameter ~9 cm. The thickness of the horn sheath was irregular, ranging from 20 mm at the proximal end to 2 mm at the distal end. The horns had grown in a spiral fashion, with ridges on the surface corresponding to seasonal growth spurts. The horns were estimated to be 6–8 years old; however, we do not know how much time had elapsed between the harvesting of the horns and our mechanical testing. Fig. 2(a) shows a photograph of the horn, and it can be seen that it is not solid, but has a hollow interior. The microstructure of the horn was characterized by optical microscopy and scanning electron microscopy (SEM). Optical micrographs were taken using Zeiss Axio imager equipped with CCD camera (Zeiss MicroImaging Inc., Thornwood, New York, USA). Porosity measurements were conducted by analyzing optical micrographs of the cross-section of the horn using the ImageJ software (a public domain, Java-based image processing program developed at the National Institutes of Health, Bethesda, MD). A field emission scanning electron microscope equipped for energy-dispersive spectroscopy (EDS) (FEI-XL30, FEI Company, Oregon, USA) was used. Samples were mounted on aluminum sample holders, air dried for 5 min and sputter-coated with gold. Samples were observed in the secondary electron mode at 20 kV accelerating voltage. Three cross-sectional areas of 300 × 250 μm^2 from different locations in the horn were scanned and element dot maps of C, O, Na, Mg, S, K and Ca were collected. X-ray diffraction (XRD) was performed on powder collected from horn by Rigaku MiniFlex™II benchtop XRD system (Rigaku Company, Texas, USA). Samples used for mechanical tests were obtained from the proximal and central (catching arch) regions of the horn where it is thickest.

For bending tests, samples were cut into rectangular prisms of dimensions 30 mm × 8 mm × 3 mm (length × width × thickness) with a diamond saw and sanded with 2400 grit sandpaper. The removal of the outer layer (with ridges) might affect the measured properties, but, due to the uneven surface, this material was not tested. Following the ASTM D790–07 standard [35], the length/width ratio was maintained at 3.75. Thirty pieces were cut to prepare two sets of samples, one called longitudinal and one called transverse. Fig. 2(b) shows the orientation of the samples for both bending and compression tests. The longitudinal samples were cut with their length parallel to the growth direction of the horn (longitudinal direction, proximal distal), with the thickness parallel to the radial direction (medial lateral). The horn was too thin to cut bending test samples in the radial direction. The transverse samples were oriented so that the long axis was perpendicular to both radial and longitudinal directions, and cut across the horn sheath.

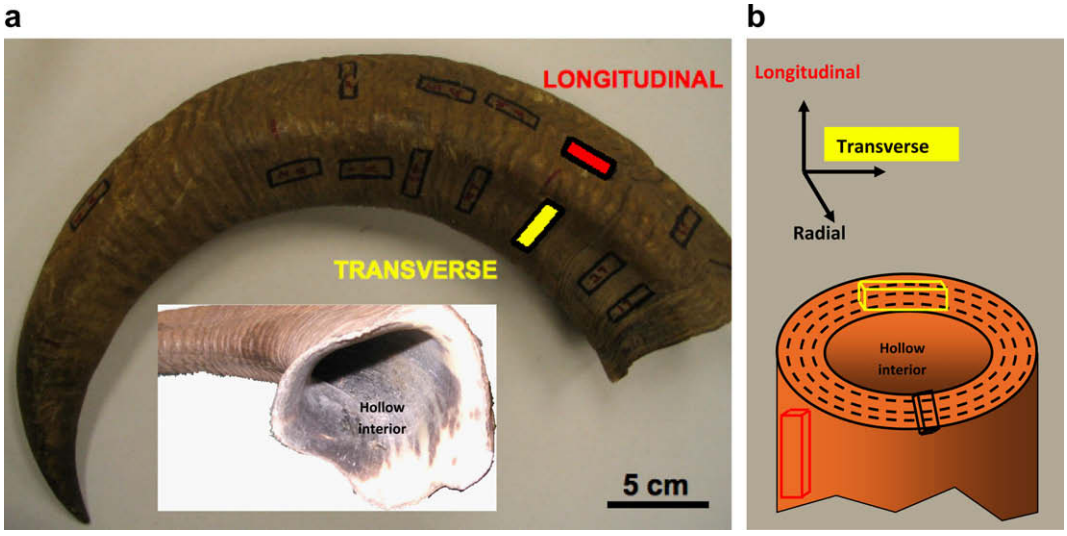

Fig. 2. Orientation of the samples cut from the horn. The inset shows the sample orientation for the bending and compression tests (not to scale).

Each set of samples was further classified into two groups: ambient dried (20 samples) and rehydrated (10 samples) conditions. The rehydrated samples were kept wet until testing. Ambient dried samples had a moisture content of 10.6 ± 0.6 wt.% water. Hydration was accomplished by immersion in tap water at room temperature for 72 h, which yielded a moisture content of 34.5 ± 2.1 wt.% water. The moisture content of the horn was calculated as the weight change after oven drying, using the procedure reported for oryx horn [29], in which oven drying at 110 °C for 24 h resulted in a moisture content of 0 wt.% water. The moisture content of a horn on a living desert bighorn sheep is not known. Kitchener and Vincent [28] found a moisture content of 20 wt.% water in fresh oryx horn. Although it would be optimal to test the horn under physiological conditions, partial hydration would result in water located in two indistinguishable places: the tubules and the keratin matrix. Thus, we tested the horn under two controllable conditions: ambient air dried and fully rehydrated.

The three-point bending tests were performed on a laboratory-designed fixture, consisting of three knife edges, such that the specimen was placed on top of two knife edges with a span of 20 mm while the third knife edge applied load to the top. A universal testing machine (Instron 3342 Single Column Testing Systems, Instron, MA, USA) equipped with a 500 N load cell was used. The crosshead speed was maintained at 0.3 mm min^{-1}, which corresponded to a strain rate of 1.5×10^{-4} s^{-1}. All samples in the ambient dried condition were tested to fracture. The fracture surface was examined using a scanning electron microscope. Samples in the rehydrated condition did not fracture; rather, they bent to extreme degrees.

For compression tests, rectangular prisms of dimensions 7.5 mm × 5 mm × 5 mm (length × width × thickness) were prepared. The samples were cut first with a handsaw and subsequently with a circular diamond blade to a length/width ratio of 1.5, with the most parallel surfaces as possible. Three sets of samples were prepared with the long axis parallel to the longitudinal, transverse or radial directions. A total of 60 samples were cut from the horn – 10 in the longitudinal direction, 10 in the transverse direction and 10 in the radial direction – for testing ambient dried horn. A similar set was prepared for the rehydrated horn, which were kept wet until testing. Compression test experiments were conducted on a universal testing machine equipped with a 30 kN load cell (Instron 3367 Dual Column Testing Systems, Instron, MA, USA). Specimens were tested at a 0.03 mm min^{-1} crosshead speed, which corresponded to a strain rate of 1×10^{-4} s^{-1}, close to the value of the bending tests. The toughness was calculated as the area under the stress–strain curves up to 60% strain, which excluded the densification area at higher strains.

It should be noted that for both the bending and the compression tests the strain rate was lower than the strain the horn would have undergone during clashing. The effect of strain rate on the mechanical properties of sheep horn was studied by Trim and Horstemeyer [36], who found that, as the strain rate increased, the Young's modulus and maximum strength increased but the toughness decreased, similar to what is found for other polymeric materials. Under high strain rate conditions, the keratin molecules do not have time to rearrange into a lower-energy configuration and thus behave as a more brittle network polymer. Other groups have tested bone (collagen matrix) that shows similar trends [37,38].

4. Results and discussion

Optical micrographs of transverse and longitudinal sections of the horn are shown in Fig. 3. The transverse section in Fig. 3(a) shows a lamellar structure with elliptically shaped porosity interspersed between the lamellae. The lamellae are ~2–5 μm thick,

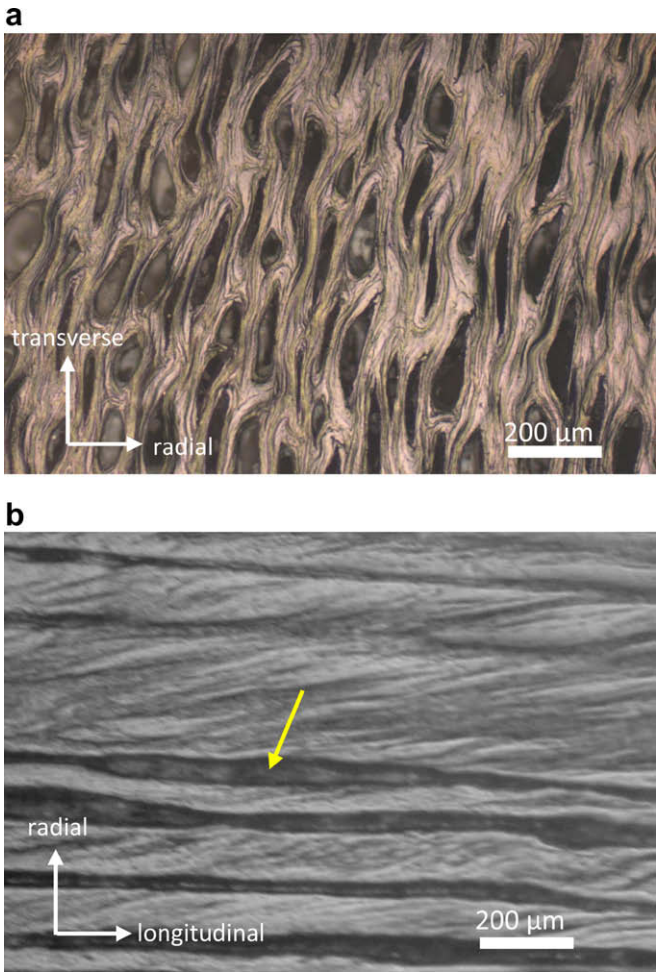

Fig. 3. Optical micrographs of the ambient dried horn. (a) Cross-section showing dark, elliptical tubules and (b) longitudinal section showing the outline of the parallel tubules (yellow arrow points to a tubule). (For interpretation of the references to colour in this figure legend, the reader is referred to the web version of this article.)

with the pore sizes ranging from 60 to 200 μm along the long axis of the pores. This porosity results from the presence of tubules that extend along the length of the horn, as shown in the longitudinal section in Fig. 3(b). The lamellae are aligned in the tubule direction and stacked in the radial direction, which creates a wavy pattern surrounding the tubules. From other optical micrographs, it appears that most of the tubules extend through the length of the horn – no terminal points were found. The porosity across the thickness of the horn was found to vary: at the outer surface (exposed to environment) the porosity ranged from 8% to 12% and decreased towards the inner surface to virtually 0%, with an overall porosity of ~7%. This gradient in porosity is similar to that found for hooves – the exterior has the greatest porosity [15]. Thus, the horn appears to be similar to hooves.

EDS analysis showed that the composition of a sample contained carbon, oxygen and sulfur, as was expected; in particular, the sulfur content suggests the presence of cysteine. The horn is a pure protein with the lack of any mineral phase. There is no significant variation in elemental content from different locations in the horn. XRD analysis of horn particles revealed that there is no crystalline phase in the horn.

The hierarchical structure of bighorn sheep horn was developed from the optical and scanning electron microscope studies, and is shown in Fig. 4. At the lowest level, the α-keratin assembles to

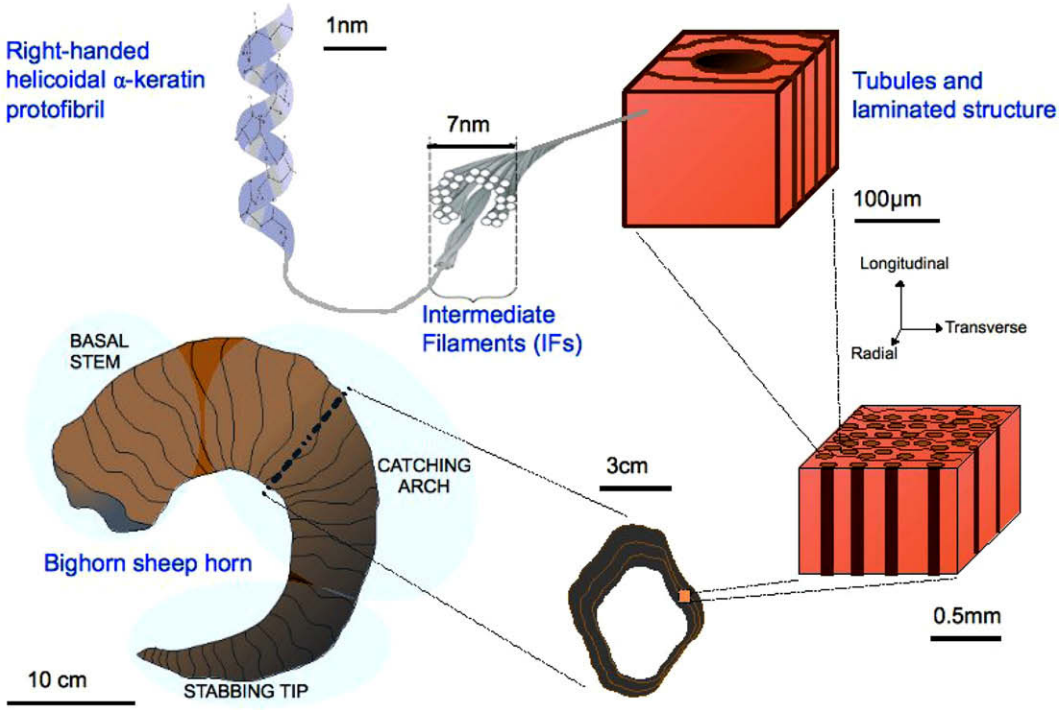

Fig. 4. Hierarchical structure of bighorn sheep horn. The horns show a spiral fashion, with ridges on the surface corresponding to seasonal growth spurts. The horns are composed of elliptical tubules, embedded in a dense laminar structure. Each lamina has oriented keratin filaments interspersed in a protein-based matrix. These filaments are two-strand coiled-coil rope polypeptide chains (intermediate filament types I and II) helically wound to form "superhelical" ropes 7 nm in diameter.

form the IFs [21], which are embedded in a protein matrix, thus forming the lamellae. These lamellae are flat sheets that are held together by other proteinaceous substances. Long tubules extend the length of the horn interspersed between the lamella. The resulting structure is a three-dimensional, laminated composite that consists of fibrous keratin and has a porosity gradient across the thickness of the horn. The presence of the tubules is surprising when considering that the horn is a laminate. Bending results in shear stresses in the horn, which would promote delamination and eventual failure. The tubules present natural regions of delamination, areas of weakness from which delamination cracks could propagate.

The three-point bending tests were conducted for both ambient dried and rehydrated conditions in longitudinal and transverse directions. No significant differences were noted between samples tested from proximal and central regions. The flexure stress is given by:

$$\sigma = \frac{3PL}{2bd^2}$$

where P is the applied load, L is the span, b is the specimen width and d is the specimen thickness.

Fig. 5 summarizes the results of the three-point bending tests. Fig. 6 shows the average three-point bending stress–strain curve for ambient dried and rehydrated conditions in the longitudinal and transverse directions. Although the above equation is not strictly valid after the samples have yielded, we show the behavior above the yield strength for comparative purposes between orientations and hydration levels. The ambient dried samples have a significantly higher elastic modulus and maximum bending strength than the rehydrated samples. In the ambient dried samples, there is a long plastic region with strains to failure of 14% and 12% for the longitudinal and transverse directions, respectively. The longitudinal and transverse elastic moduli are similar, indicative that any alignment of the keratin fibers does not have a significant effect. This is in agreement with the findings of Kasapi and Gosline for equine hooves [10,11]. The elastic moduli values are also in good agreement with Kitchener and Vincent [28], who found the modulus to vary from 1.8 to 6.1 GPa for 40 to 0 wt.% water in the oryx horn. Our values range from 0.63 to 2.20 GPa for 34.5 to 10.6 wt.% water. These values are also in the range of what was reported for sheep horn by Warburton [30]: an elastic modulus of 1.5 GPa for 20 wt.% water.

The bending strength is higher for the longitudinal samples compared with the transverse samples. In the longitudinal direction, the load is applied perpendicular to the tubule direction, while in the transverse direction it is applied parallel to the tubule direction (Fig. 6). Delamination is more facile in the transverse direction, due to the natural separation of the lamellae from the tubules.

The fracture surface of a transverse specimen shows the fibrous and lamellar nature of the horn, as seen in Fig. 7. The small fibers are IF bundles, which are arranged into the lamellae. Delamination is evident (Fig. 7 on the right) along with IF fracture. The most significant effect on the horn keratin is the presence of water, far beyond any IF alignment issues – an effect that is also found for hoof keratin [13] and oryx horn [29]. The significance of hydration is also observed in another biological material, bone. Dry bone is brittle and has low fracture resistance, whereas hydrated bone has over twice the fracture toughness [39].

For rehydrated bending samples, the elastic modulus and maximum bending strength was found to be approximately the same in both the longitudinal and transverse directions. The strong similarity between the mechanical properties suggests that hydration severely degraded the matrix phase, which then dominated the deformation behavior, in accordance with the plasticizing effect of increasing water content in the matrix [23,29]. The samples deformed over 20% but none broke in half. Interestingly, the deformed samples recovered their initial shape after ~1 h at room temperature, indicating a short recovery time for the rehydrated

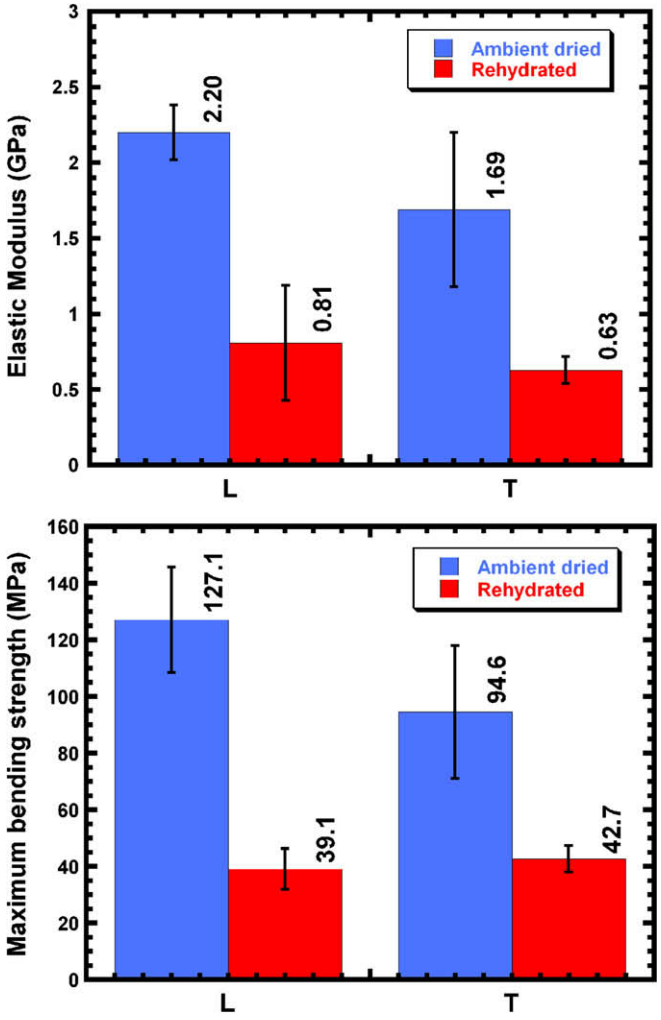

Fig. 5. Elastic modulus and maximum bending strength determined by three-point tests of ambient dried and rehydrated horn specimens in the longitudinal (L) and transverse (T) directions. $n = 10$ for all data sets.

matrix phase [29]. An optical micrograph of the central region of a rehydrated sample taken after recovery from a bend test is shown in Fig. 8(a). According to Kitchener [29], a delamination toughening mechanism was found in the horns after three-point bending tests. Delamination is evident in our samples in the region where the shear stress is maximum (half the sample thickness). In addition, ligament bridging is also observed, which further enhances the fracture resistance. Although we tested only one pair of horns, preliminary results on another set of horns show similar microstructural features and mechanical property measurements.

SEM micrographs of a fracture surface from an ambient dried sample after three-point bending test in the longitudinal direction is shown in Fig. 8(b). The elliptical (40 μm × 100 μm) tubule cross-section is more rounded than what is shown in Fig. 3. The dissimilarities can be ascribed to the following factors: the images were taken from different regions of the horn, where the porosity was not the same; and Fig. 3 was taken from a flat, polished surface whereas Fig. 8(b) is from a fracture surface, which is unlikely to be oriented so that the surface is exactly perpendicular to the longitudinal axis. The tubules give the impression that there are concentric rings surrounding the main channel, but no definite "tubular" or "intertubular" regions are observed. The circular lamellar structure around the tubules suggests that the horn structure is similar to that of hooves and rhinoceros horn.

The compression tests were conducted for each direction (longitudinal, transverse and radial) in ambient dried and rehydrated conditions. Fig. 9 summarizes the results for the compression tests, and the stress–strain curves are shown in Fig. 10. Different maximum strains (from 10% to 70%) were tested in each direction in order to evaluate the microstructure after the test at different steps of deformation. Although the horn would not normally be subjected to such high strains, the fracture behavior and failure mechanisms can be observed more clearly at these values. In the ambient dried condition, the elastic modulus and yield strength are similar for both the longitudinal and transverse samples. The yield strength is taken as the intersection of a line drawn parallel to the elastic region of the stress–strain curve at 0.2% strain. The elastic modulus and yield strength is lowest in the radial direction. In the longitudinal and transverse directions the lamellae are parallel to the loading direction, whereas in the radial direction the lamellae are perpendicular. Thus, some of the stress applied in the radial direction is expended to close the tubules. For all samples, after the linear elastic region there is a large plastic region, indicating extensive damage accumulation. At strains greater than ~60%, the samples experienced crushing densification. The rehydrated compression samples showed a similar trend to the ambient dried samples, although the values are much lower.

Toughness values for the ambient dried samples ranged from 56 MJ m^{-3} for the longitudinal and transverse directions to 74 MJ m^{-3} for the radial direction. For rehydrated samples the toughness was found to be lower, but the trend was the same as for ambient dried conditions: the toughness in the transverse and longitudinal directions was lower (12 MJ m^{-3}) than in the radial direction (18 MJ m^{-3}). Because the horn showed a structure comprising lamellae stacked in the plane perpendicular to the radial direction, the toughness was found to be the same for the samples tested in both the longitudinal and transverse directions. The higher toughness found in samples tested in the radial direction is most likely associated with the energy absorption by compression of the tubules. This is the orientation in which horns clash during combat.

Fig. 11 shows optical micrographs of the damage incurred by the compression test samples in the ambient dried condition. In the longitudinal direction, compression results in first delamination and then microbuckling of the lamellae. Because the lamellae are not perfectly aligned in the longitudinal direction, local stress concentrators can arise that will cause microbuckling, or kinking, of the lamella when compressed in the longitudinal direction. Large delamination voids arise due to eventual barreling of the samples. Lamellae are not perfectly aligned in the transverse direction either, because they surround the irregularly shaped tubules. At 30% strain, lamellar buckling is observed in the wavy pattern of the lamellae. At 60% strain the microbuckling has fully or partially closed the tubules, creating a cross-shaped void. For the radial direction, the tubules are squeezed and the lamellae are aligned more in a direction perpendicular to the applied load. At 60% strain, the tubules are almost completely closed, and it appears that some of the long pores in the 30% strain micrograph are squeezed in the middle and separate into smaller pores. Delamination or microbuckling is not evident. These deformation patterns attest to the two-dimensional laminated structure of the horn.

Table 2 presents the microstructural features of different keratinized structural materials, estimated from calculated values or micrographs. The pore size is the medullary cavity size in hoof and rhinoceros horn, and the tubule diameter in the sheep horn. The diameters are similar, all <100 μm and >20 μm. The density of the tubules is highest in the bovine hoof and lowest in the rhinoceros horn, with the sheep horn falling midrange.

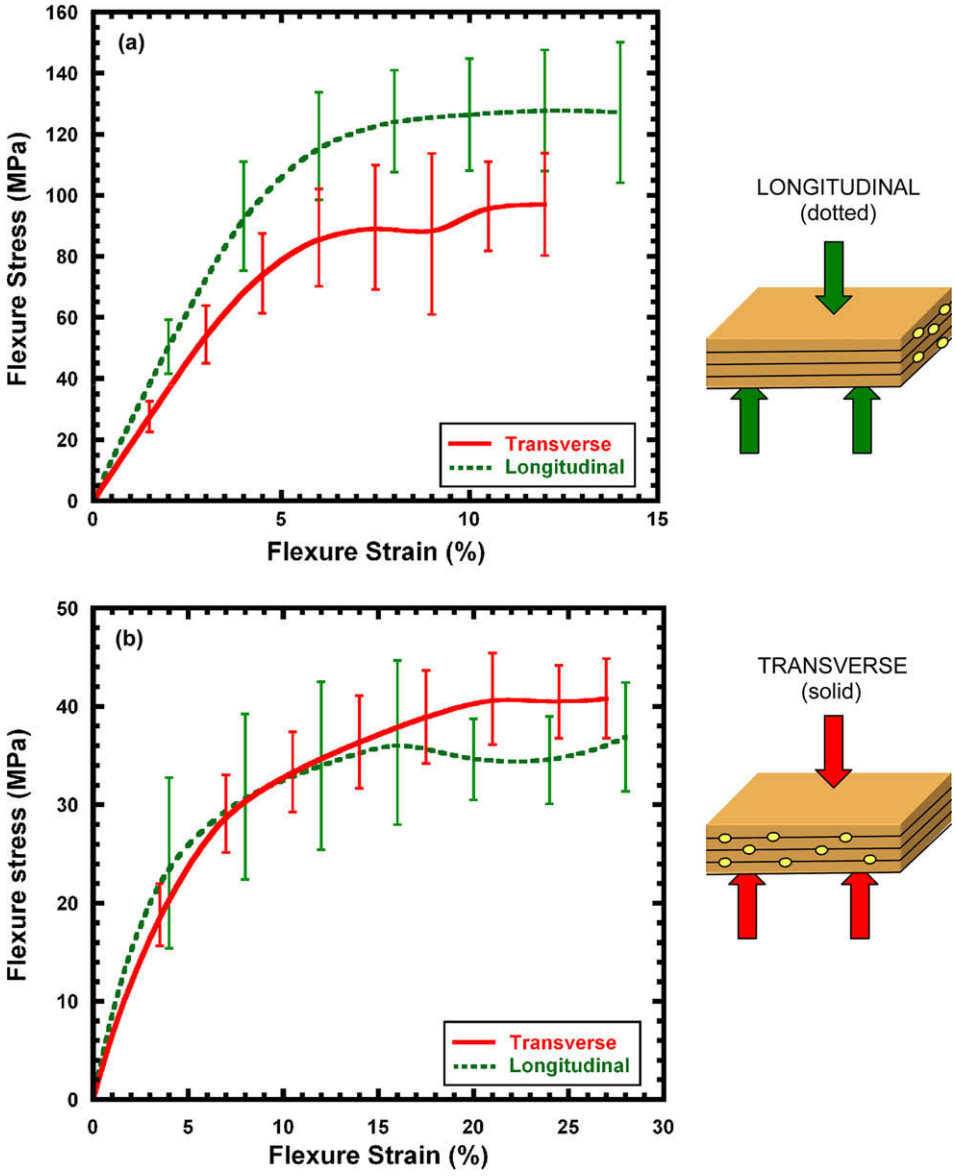

Fig. 6. Average stress–strain curve of (a) ambient dried and (b) rehydrated horn for the three-point bending test in the longitudinal and transverse directions.

There is a gradient of porosity in the hooves and horns, with the highest porosity occurring at the exterior compared with the interior. Even though there are questions about what specific mechanical role (or roles) the hollow tubules play in the hoof wall, it is widely accepted that they serve mechanical functions such as toughening by crack deflection. The tubules prevent cooperative buckling of the structure by increasing the resistance to compressive failure of the wall [15]. The similarity in the porosity gradient between hooves and horns is not totally unexpected because both hooves and horns serve the primary role of transmitting the reaction forces to the bony skeleton. Furthermore, they both undergo impact forces (during galloping and clashing, respectively) and are both loaded in bending and compression [15,25]. Finally, in comparison to other biological materials, such as bone, horn has the highest work of fracture and toughness, and rivals values found for synthetic polymers and polymer composites. The unique deformation mechanisms (delamination, microbuckling of the laminates and tubule collapse) contribute to the enhanced toughness. It appears that the horn and hoof structures are ideal designs for impact resistance and energy absorption [13,20].

5. Conclusions

The microstructure and mechanical properties (bending and compression) in ambient dried and rehydrated conditions of bighorn sheep (*Ovis canadensis*) horns were investigated. The main findings are:

- Horn is a composite material consisting of stacked lamellae in the radial direction with a thickness of 2–5 μm, with tubules, ~40 × 100 μm in diameter, interspersed between the lamellae. This results in an overall cross-sectional porosity of 7%.
- There is a gradient in porosity across the thickness of the horn – the porosity decreases from the external surface (8–12%) to the interior surface (~0%). This is similar to what is observed in hooves.
- Rehydration has a significant effect on reducing the maximum bending strength and elastic modulus of the horn, more so than the effect of sample orientation. There is no significant difference between the elastic modulus and the maximum bending strength in the longitudinal or transverse directions for the

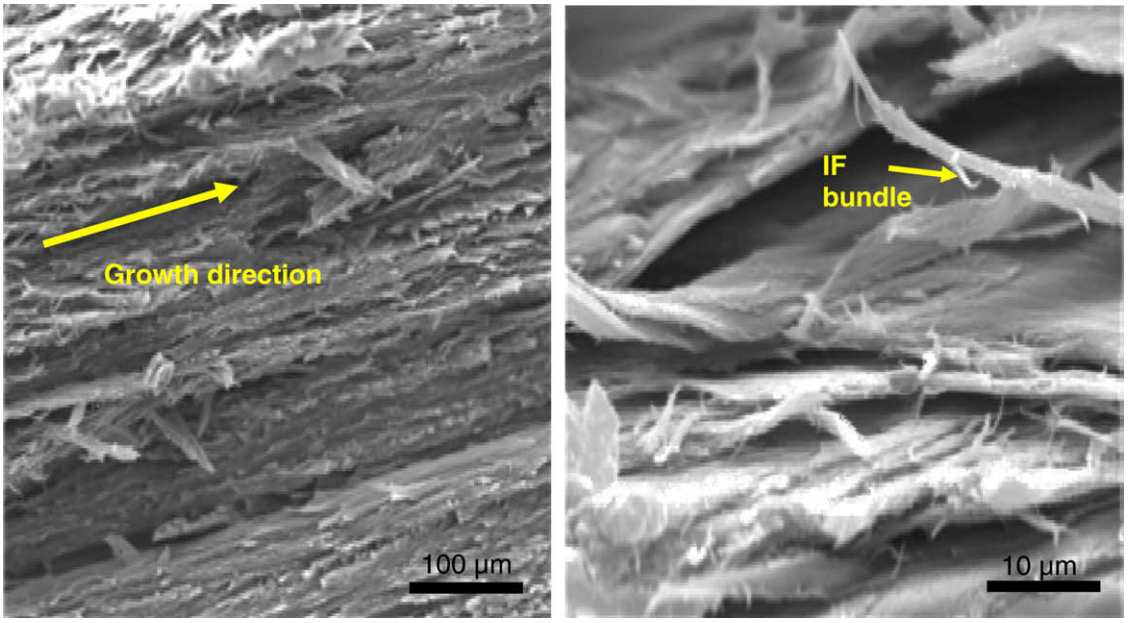

Fig. 7. SEM micrographs of the fracture surface of the transversely oriented samples tested in three-point bending. Micrographs show the fibrous and laminar nature of bighorn sheep horn microstructure. The lamellae are aligned in the growth direction of the horns.

rehydrated specimens, suggesting that the weakened matrix dominates the mechanical performance.

- Fracture micrographs from bend tests show delamination, ligament bridging and intermediate filament fracture as the main failure modes.
- Compression tests revealed that the elastic modulus and yield strength of the ambient dried samples in the longitudinal and

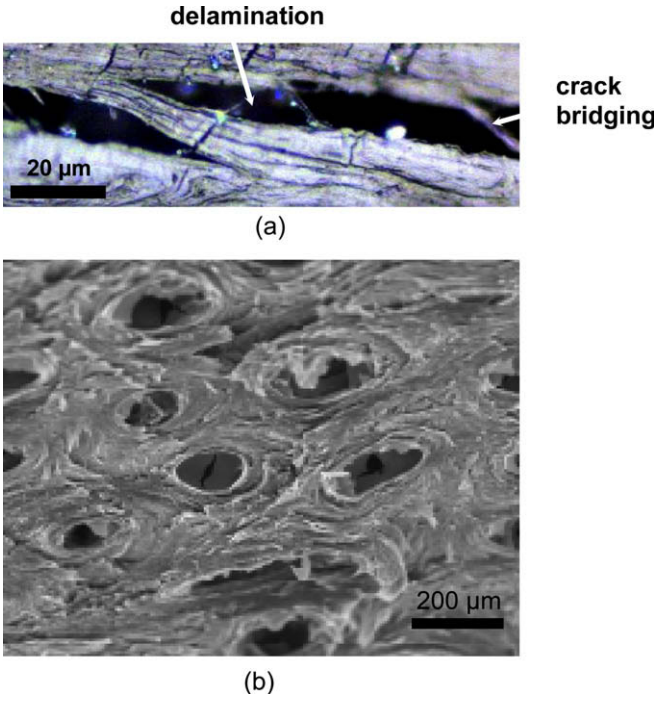

Fig. 8. (a) Optical micrograph taken from the central region of the rehydrated samples tested in three-point bending in the longitudinal direction. Toughening mechanisms of delamination and crack bridging are observed. (b) SEM micrographs of the three-point bending test fracture surface from a longitudinally oriented sample in ambient dried conditions. The microstructure is characterized by numerous tubules, with concentric rings surrounding them.

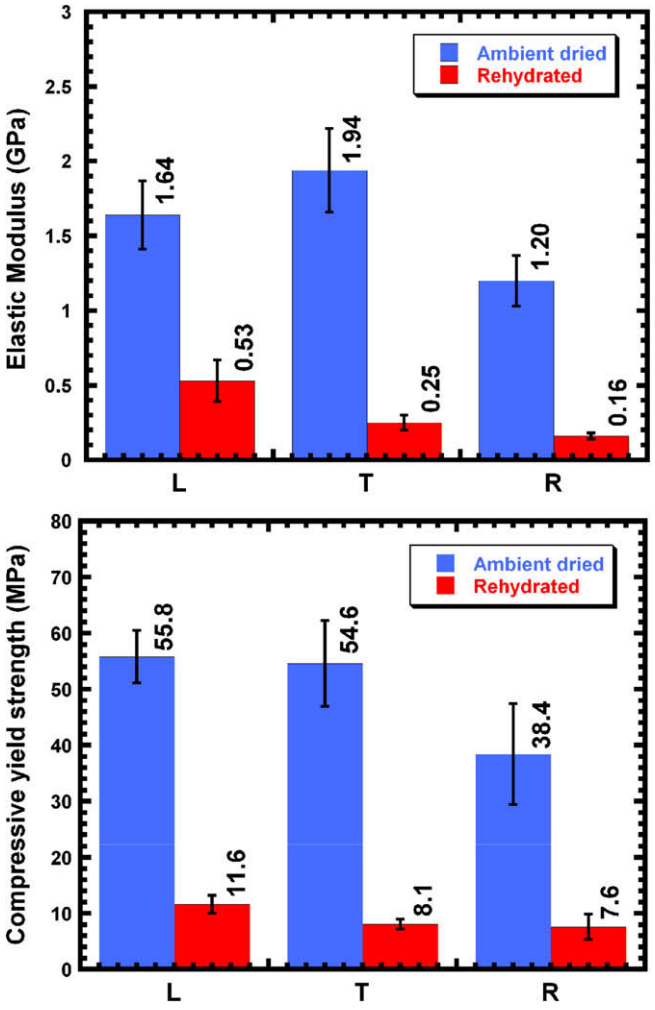

Fig. 9. Elastic modulus and yield strength determined by compression tests for ambient dried and rehydrated horn specimens in the longitudinal (L), transverse (T) and radial (R) directions. $n = 10$ for all data sets.

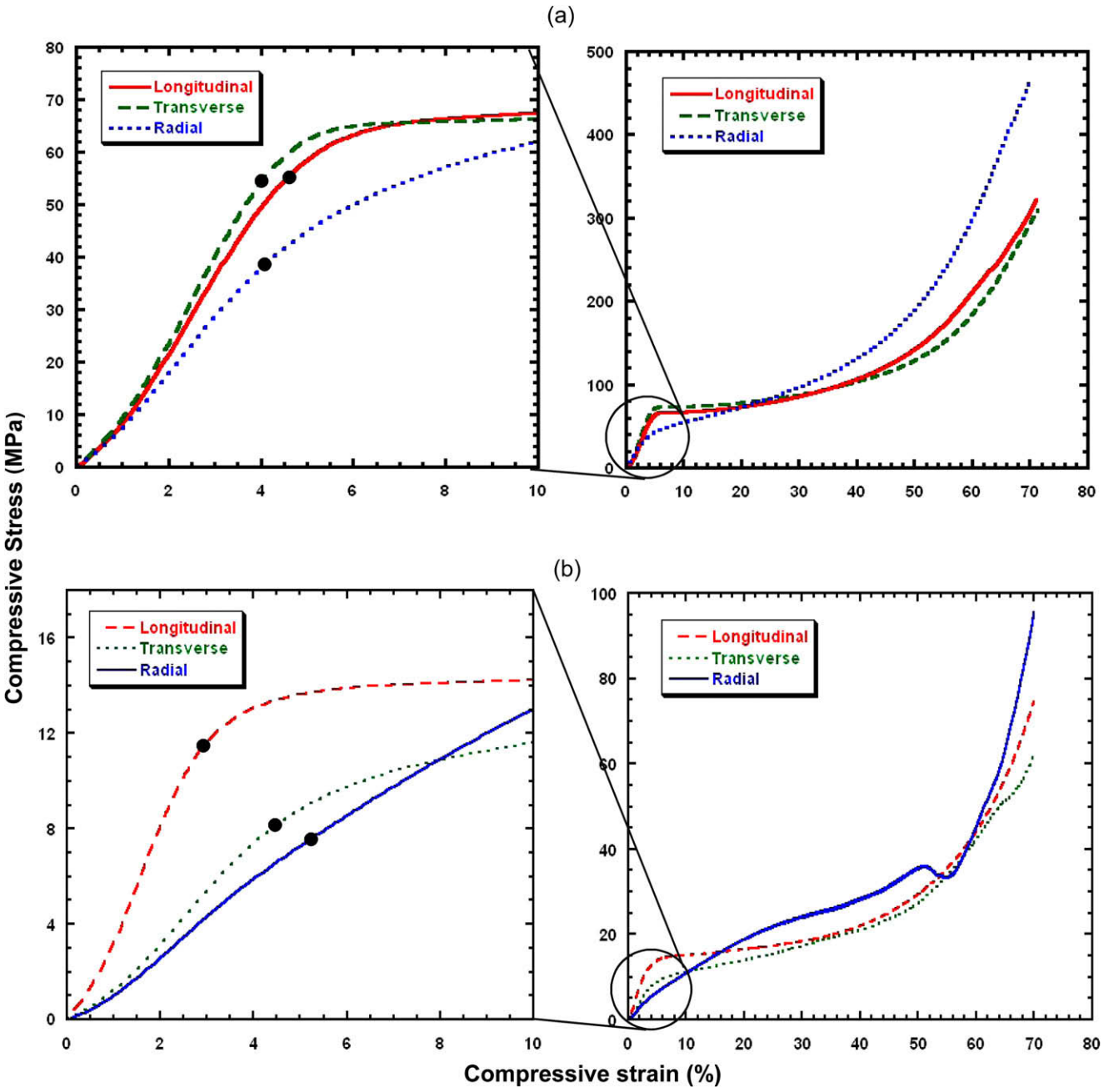

Fig. 10. Compressive stress–strain curve for (a) ambient dried and (b) rehydrated conditions. The figures on the left magnify the low strain region. The black dot identifies the 0.2% strain offset yield point.

transverse directions were the same. The elastic modulus and yield strength of the radial samples were smaller, owing to the ease of compressing the tubules. Hydration degraded the elastic modulus and strength.

- Due to the laminated structure of the horn, compression tests for the ambient dried condition revealed that the toughness was the same in the longitudinal and transverse directions but higher in the radial direction. In the radial direction, compression of the tubules aids in energy absorption. The toughness was lower for the rehydrated condition, but the trend with the orientation was the same.
- This is the first study to report on the deformation mechanisms in compression, such as delamination and microbuckling of the lamellae in the longitudinal and transverse directions as the main sources of failure. Extensive tubule collapse was found for samples tested in compression in the radial direction, which enhanced the toughness.

Acknowledgements

We thank Ryan Anderson of the Nano3 Laboratory of CalIt2 for helping with the SEM, Jonathan Tao for collecting the XRD data and Professor Marc A. Meyers for his enthusiastic support of this project. This work was supported by the National Science Foundation, Division of Materials Research, Biomaterials Program (Grant DMR 0510138) and the Army Research Office (Grant W911-08-1-0461).

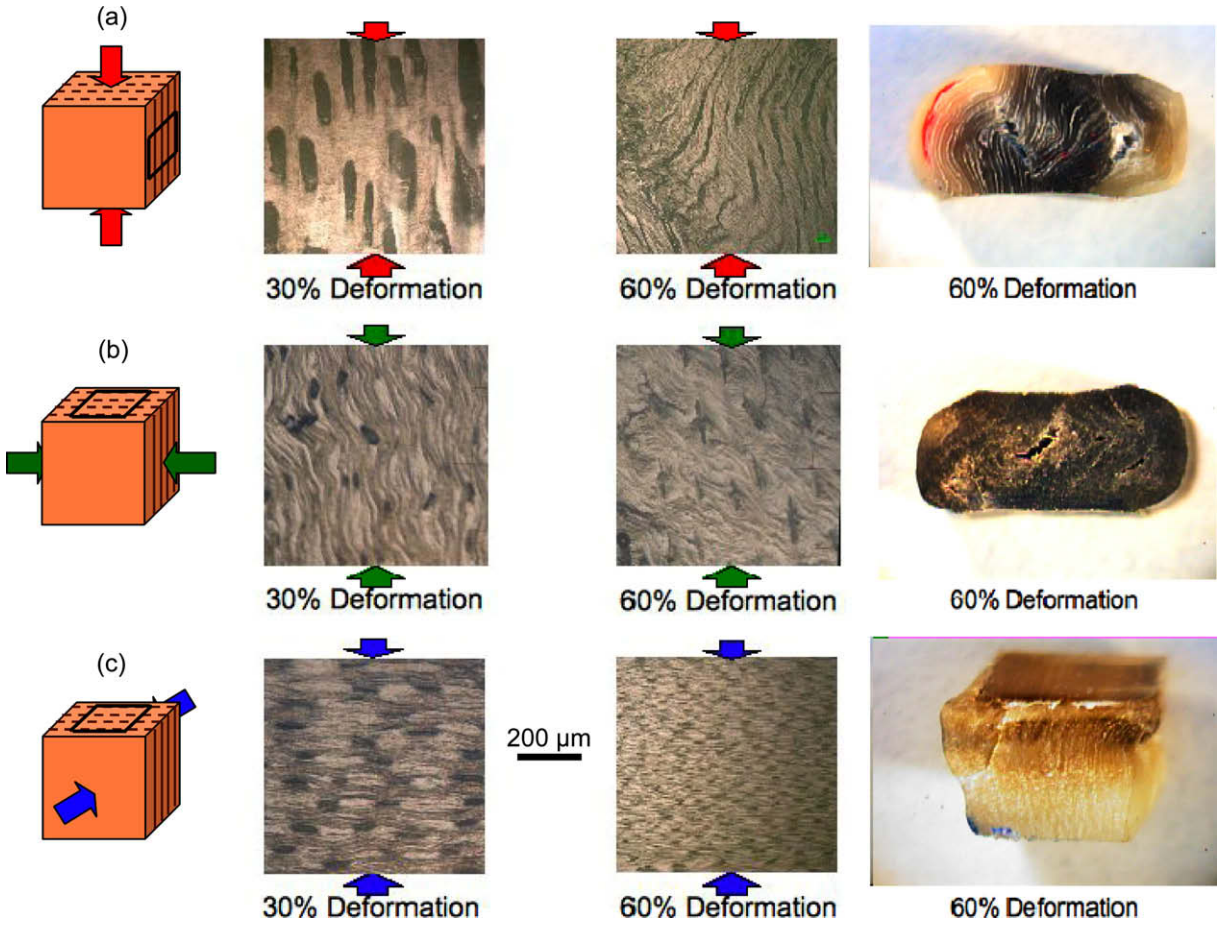

Fig. 11. Optical micrographs of the deformation of ambient dried horn at 30 and 60% strain for the (a) longitudinal, (b) transverse and (c) radial directions. Pictures on the right show the accumulated damage in the samples.

Table 2
Comparison of the microstructural features in different keratinized structures.

	Tubule diameter (μm)	Average pore diameter (μm)	Average tubule density (mm^{-2})	Average porosity (%)	Ref.
Horn					
Rhinoceros	300–500	20 × 60	7*	<1**	[33,34]
Sheep		100 × 40	22	7	This work
Hoof					
Bovine	20 × 45	20 × 10***	59	<1**	[12]
Equine	218 × 142**	48**	16++	2+	[10]

* Estimated from a picture in Ref. [33].
** Calculated from the reference.
*** Estimated from a micrograph in Ref. [12].
\+ Estimated from a micrograph in Ref. [15].
\++ Estimated from a micrograph in Ref. [48].

Appendix A

Figures with essential colour discrimination. Certain figures in this article, particularly Figs. 1–11, are difficult to interpret in black and white. The full colour images can be found in the on-line version, at doi:10.1016/j.actbio.2009.06.033.

References

[1] Currey JD. Physical characteristics affecting the tensile failure properties of compact bone. J Biomech 1990;23:837–44.
[2] Spatz H-CH, O'Leary EJ, Vincent JFV. Young's moduli and shear moduli in cortical bone. Proc R Soc Lond 1996;263:287–94.
[3] Vashishth D, Behiri JC, Bonfield W. Crack growth resistance in cortical bone: concept of microcrack toughening. J Biomech 1997;30:763–9.
[4] Jameson MW, Hood JAA, Tidmarsh BG. The effects of dehydration and rehydration on some mechanical properties of human dentin. J Biomech 1993;26:1055–65.
[5] Marshall GW, Balooch M, Gallagher RR, Gansky SA, Marshall SJ. Mechanical properties of the dentin/enamel junction: AFM studies of nanohardness, elastic modulus, and fracture. J Biomed Mater Res 2001;54:87–95.
[6] Currey JD. Mechanical properties of mollusk shell. In: Vincent JFV, Currey JD, editors. The mechanical properties of biological materials. Symposium of the society of experimental biology. Cambridge: Cambridge University Press; 1980. p. 75–9.
[7] Jackson AP, Vincent JFV, Turner RM. The mechanical design of nacre. Proc R Soc Lond B 1998;234:415–40.
[8] Menig R, Meyers MH, Meyers MA, Vecchio KS. Quasi-static and dynamic mechanical response of Haliotis rufescens (abalone) shells. Acta Mater 2000;48:2383–98.
[9] Bertram JEA, Gosline JM. Fracture toughness design in horse hoof keratin. J Exp Biol 1986;125:29–47.
[10] Kasapi MA, Gosline JM. Design complexity and fracture control in the equine hoof wall. J Exp Biol 1997;200:1639–59.
[11] Kasapi MA, Gosline JM. Micromechanics of the equine hoof wall: optimizing crack control and material stiffness through modulation of the properties of keratin. J Exp Biol 1999;202:377–91.
[12] Franck A, Cocquyt G, Simoens P, De Belie N. Biomechanical properties of bovine claw horn. Biosys Eng 2006;93:459–67.
[13] Bertram JEA, Gosline JM. Functional design of horse hoof keratin: the modulation of mechanical properties through hydration effects. J Exp Biol 1987;130:121–36.
[14] Clark C, Petrie L. Fracture toughness of bovine claw horn cattle with and without vertical fissures. Vet J 2007;173:541–7.
[15] Kasapi MA, Gosline JM. Exploring the possible functions of equine hoof wall tubules. Equine Vet J 1998;26:10–4.
[16] Baillie C, Southam C, Buxtin A, Pavan P. Structure and properties of bovine hoof horn. Appl Compos Lett 2000;9:107–15.

[17] Bendit EG, Kelly M. Properties of the matrix in keratins. Part I: The compression technique. Text Res J 1978;48:674–9.
[18] Meyers MA, Chen PY, Lin AYM, Seki Y. Biological materials: structure and mechanical properties. Prog Mater Sci 2008;53:1–206.
[19] Chen PY, Lin AYM, Seki YS, Stokes AG, Peyras J, Olevsky EA, et al. Structure and mechanical properties of selected biological materials. J Mech Behav Biomed Mater 2008;1:208–26.
[20] Kitchener AC. Fighting and the mechanical design of horns and antlers. In: Domenici P, Blake RW, editors. Biomechanics in animal behaviour. Oxford: BIOS Scientific Publishers; 2000.
[21] Fraser RD, MacRae TP, Parry DA, Suzuki E. Intermediate filaments in alpha keratins. Proc Natl Acad Sci USA 1986;83:1179–83.
[22] Fraser RD, MacRae TP. Molecular structure and mechanical properties of keratin. In: Vincent JFV, Currey JD, editors. The mechanical properties of biological materials. Symposium of the society of experimental biology. Cambridge: Cambridge University Press; 1980. p. 211–46.
[23] Feughelman M. Mechanical properties and structure of α-keratin fibres: wool, human hair and related fibres. Sydney: University of New South Wales Press; 1997.
[24] Makinson KR. The elastic anisotropy of keratinous solids. Aust J Exp Biol Med Sci 1954;7:336–47.
[25] Kitchener AC. The evolution and mechanical design of horns and antlers. In: Rayner JMV, Wootton RJ, editors. Biomechanics and Evolution. Cambridge: Cambridge University Press; 1991.
[26] Kitchener A. An analysis of the forces of fighting of the blackbuck (*Antilope cervicapra*) and the bighorn sheep (*Ovis canadensis*) and the mechanical design of horns of bovids. J Zool 1988;214:1–20.
[27] Kitchener A. Fracture toughness of horns and a reinterpretation of the horning behaviour of bovids. J Zool 1987;213:621–39.
[28] Kitchener A, Vincent JFV. Composite theory and the effect of water on the stiffness of horn keratin. J Mater Sci 1987;22:1385–9.
[29] Kitchener A. Effect of water on the linear viscoelasticity of horn sheath keratin. J Mater Sci Lett 1987;6:321–2.
[30] Warburton FL. Determination of the elastic properties of horn keratin. J Text Inst 1948;39:297–307.
[31] Vincent JFV. Structural biomaterials. revised ed. Priceton, NJ: Princeton University Press; 1982.
[32] Baillie C, Fitford R. The three-dimensional composite structure of cow hoof wall. Biomimetics 1996;4:1–22.
[33] Ryder ML. Structure of the rhinoceros horn. Nature 1962;193:1199–201.
[34] Hieronymus TL, Witmer LM, Ridgely RC. Structure of white rhinoceros (*Ceratotherium simum*) horn Investigated by X-ray computed tomography and histology with implications for growth and external form. J Morphol 2006;267:1172–6.
[35] ASTM D790-07, Standard test methods for flexural properties of unreinforced and reinforced plastics and electrical insulating materials.
[36] Trim WE, Horstemeyer ME. Unpublished results.
[37] McElhaney JH. Dynamic response of bone and muscle tissue. J Appl Physiol 1966;21:1231–6.
[38] Adharapurapu RR, Jiang F, Vecchio KS. Dynamic fracture of bovine bone. Mater Sci Eng C 2006;26:1325–32.
[39] Chen PY, Stokes AG, McKittrick J. Comparison of the structure and mechanical properties of bovine femur bone and antler of the North American elk (*Cervus elaphus canadensis*). Acta Biomater 2008;5:693–706.
[40] Wagner IP, Hood DM, Hogan HA. Comparison of bending modulus and yield strength between outer stratum medium and stratum medium zone alba in equine hooves. Am J Vet Res 2001;62:745–51.
[41] Currey JD. The design of mineralized hard tissues for their mechanical functions. J Exp Biol 1999;202:3285–94.
[42] Currey JD. Mechanical properties of bone tissues with greatly differing functions. J Biomech 1979;12:313–9.
[43] Lin AYM, Meyers MA, Vecchio KS. Mechanical properties and structure of *Strombus gigas*, *Tridacna gigas* and *Haliotis rufescens* sea shells: a comparative study. Mat Sci Eng C 2006;26:1380–9.
[44] Fila M, Bredin C, Piggott MR. Work of fracture of fibre-reinforced polymers. J Mater Sci 1972;7:983–8.
[45] Callister WD. Materials science and engineering: an introduction. New York: John Wiley & Sons; 2007. p. 594.
[46] Hashemi S. Temperature and deformation rate dependence of the work of fracture in polycarbonate (PC) film. J Mater Sci 2000:5851–6.
[47] Petrie SP, DiBenedetto AT, Miltz J. Effects of the state of stress on the toughness of polycarbonate. Polym Eng Sci 1978;18:1200–8.
[48] Reilly JD, Collins SN, Cope BC, Hopegood L, Lathan RJ. Tubule density of the stratum medium of horse hoof. Equine Vet J 1998;26(Suppl.):4–9.